

NUMERICAL SIMULATION OF A PERIODIC ARRAY OF BUBBLES IN A CHANNEL

N. Mangiavacchi^a, G.C.P. Oliveira^a, G. Anjos^a and J. R. Thome^b

^a*Group of Environmental Studies of Hydropower Reservoirs (GESAR Lab), Faculty of Engineering, State University of Rio de Janeiro, Rio de Janeiro, Brazil norberto@uerj.br, <http://www.uerj.br>*

^b*Laboratoire de Transfert de Chaleur et de Masse (LTCM), École Polytechnique Fédéral de Lausanne, Lausanne, Switzerland john.thome@epfl.ch, <http://www.ltcem.epfl.ch>*

Keywords: Two-phase flow, finite element, bubbles, periodic boundary conditions.

Abstract. Flows in micro-channels involving bubbles have important applications in electronic and chemical devices. The numerical simulation of a periodic array of bubbles in a channel is performed using a Semi-Lagrangian Finite Element Method. Interfaces are accurately tracked employing an Arbitrary Lagrangian-Eulerian approach. The methodology for the application of the periodic boundary conditions for this problem is exploited under a finite element context through the overloading of degrees of freedom located at the periodic boundaries. A study of case is performed by considering the initialization of two Taylor bubbles equally shaped and uniformly spaced inside a two-dimensional domain (flat channel) under a moving-frame technique, using a frame moving with the mean velocity of the bubbles. Numerical results supporting the periodic implementation are presented and discussed.

1 INTRODUCTION

Geometrically periodic configurations arise in many industrial applications where fluid flows with repetitive behavior are desired. This periodic nature is found not only in flow systems operating under a cyclic way such as heat exchangers, evaporators, and condenser tubes, but also in unidirectional flows in the fully developed regime inside longitudinal channels. In the former devices, arrays of fins or plates are arranged to create periodic patterns that influence the flow and other properties of the system, (Murthy and Mathur (1997)), while two-phase flow patterns inside channels such as annular, bubbly, and slug flows, chiefly, can be treated as regular and spatially periodic under certain hypotheses (Asadolahi et al. (2011)).

Periodic boundary conditions (PBC, henceforth) have been an appreciated tool in different areas in attempting to obtain computational efficiency when either fully developed or periodic regimes are taken into account. Flows of granular material (Campbell and Brennen (1985)), fluid-particle flows (Maury (1999)), heat and mass transfer problems (Beale (2007)), and the dynamics of gas-liquid flows in long oil pipelines (Sawko and Thompson (2011)) are some examples of fields where this strategy was used. PBC are typically adopted to isolate bulk phenomena, when boundary effects of the real physical system can be neglected in relation to hydrodynamic effects that take place internally.

This work intends to develop a computational strategy to simulate two-phase flows based on a periodic array of bubbles with PBC. We use an Arbitrary Lagrangian-Eulerian/Finite Element Method (ALE/FEM) methodology developed by Anjos (2012) and recently published (Anjos et al. (2013)) to discretize the Navier-Stokes equations and simulate flows at low Reynolds numbers. Additionally, a Moving Frame (MFR) technique similar to that encountered in Talimi et al. (2012a) is integrated into the simulation framework. Along with the MFR technique, the PBC work as a complementary mechanism to reduce computational efforts and evaluate the fluid flow locally, i.e., inside a smaller computational domain. Circular, rectangular, or triangular channels, and channels with different topologies of boundary (ellipsoidal, prismatic, or more complex surfaces) obtained by geometrical translation or extrusion fit within the range of application of the PBC. Furthermore, as cited by Talimi et al. (2012b), two-phase slug flow simulations in some of these domains are still unexplored. This paper deals with the application of the PBC to a simple two-phase flow. The methodology is applied to a simple idealization of the Taylor flow (Davies and Taylor (1950)) (or slug flow), due to its high capabilities to exchange heat, mainly in applications dealing with microchannel two-phase microelectronics cooling. Nowadays, particular attention is being devoted to these fields (Gupta et al. (2009), Gupta et al. (2010), Magnini (2012)), Magnini et al. (2013)).

The paper is structured as it follows: Section 2 describes the computational domain used in the simulations as well as the governing equations; Section 3 introduces briefly the strategy to impose the PBC through FEM and discusses its implementation; Section 4 presents the numerical results for a periodic setup, and the Section 5 presents the conclusions drawn from the present work.

2 POSING THE PROBLEM

2.1 Domain of the Periodic Array

The mathematical modeling of the periodic array of bubbles is set forth as follows. Let $\Omega \subset \mathbb{R}^2$ be an open bounded set and Γ its boundary, both of which are defined as

$$\Omega := \Omega^g \cup \Omega^l, \quad \text{where } \Omega^g = \bigcup_{i=1}^{nb} \Omega_i^g, \quad \text{and} \quad (1)$$

$$\Gamma := \Gamma^g \cup \Gamma^l, \quad \text{where } \Gamma^g = \bigcup_{i=1}^{nb} \Gamma_i^g, \quad \Gamma^l = \Gamma_T \cup \Gamma_B \cup \Gamma_L \cup \Gamma_R, \quad (2)$$

respectively. Above, the superscripts g, l stand for *vapor* and *liquid* phases, nb is the number of bubbles arbitrarily set into the array, and Γ^l represents the union of solid walls (Γ_T, Γ_B) plus a pair of periodic boundaries ($\Gamma_L \cup \Gamma_R$) of a rectangular flat channel of width D . The bubbles are arranged in a row fashion inside the channel and separated by a slug of fixed length. Coalescence events are not considered in the simulation. The bubbles are initialized as a rectangle with an arched “cap” at right nose, whose total length is given by DH . In other words, elongated bubbles like those found in [Davies and Taylor \(1950\)](#) were chosen for convenience. Moreover, both the slug length and the distance from the first (or last) bubble to the beginning (or end) of the channel are set to be the half of DH .

On the other hand, the initial vertical length DV of the bubbles is computed by a correlation between the thin film thickness δ and the channel diameter D , due to [Bretherton \(1961\)](#), given by

$$\frac{\delta}{D} = 0.67Ca^{2/3}, \quad (3)$$

where

$$Ca = \frac{\mu_l u_l}{\sigma} \quad (4)$$

is the Capillary number, μ_l the dynamic viscosity of the liquid, u_l the value of the streamwise liquid velocity, and σ the surface tension. Equation 3 is used here as an initial parameter to arrange the bubbles in the array, but the interface is allowed to move with the flow. The thickness of the film at later times is obtained as a result of the simulation.

The MFR technique, which sets the velocity referential used in this paper, is similar to that used by [Talimi et al. \(2012a\)](#). The reference frame is allowed to move continuously with the mean bubble velocity u_l . MFR techniques are intended to reduce the computational cost of the simulations when slicing a long domain to obtain a “unit cell”, “simulation box”, or simply “periodic module”. Such slicing is a usual numerical approach. Although one of the goals of this work is focused on numerical simulations that seek to reduce the length of a real channel, it is worth to stress here that a number relatively big of nb can be employed to line up uniformly as much bubbles as desired for conjectural analyses. Inasmuch as the computational domain was constructed for a specific study, the channel length L is determined by

$$L = (nb)DH + (nb + 1)s, \quad nb = 1, 2, \dots \quad (5)$$

where s is the slug length. Thenceforth, there is freedom to limit or expand the number of unit cells to be used.

PBC are imposed at the inlet and outlet of the channel, whose methodology of implementation through the FEM is discussed later. Figure 1 depicts the domain described until now for

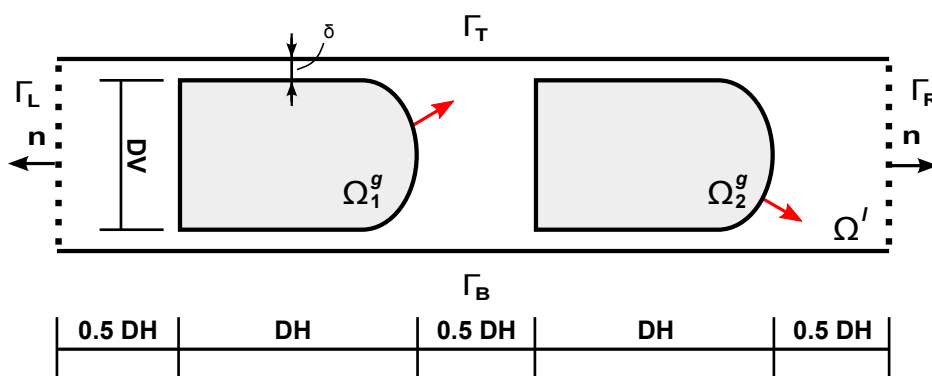


Figure 1: Domain of the periodic array of bubbles used for moving frame simulations with periodic boundary conditions.

the case $nb = 2$. The dotted boundaries are to emphasize the application of the PBC, while \mathbf{n} symbolizes their unit normal vectors pointing outward. In advance to further explanations upon the interface modeling, normal vectors in red are also drawn to specify the direction (i.e., from vapor to liquid) chosen for curvature calculations.

2.2 ALE Governing Equations

The Arbitrary Lagrangian-Eulerian (ALE) formulation to describe the movement of the fluid follows Anjos (2012) and is applied together with a decomposition of the pressure field p , which is subdivided into a part related to the local motion of the fluid and a periodic parcel and given by

$$p(\mathbf{x}, t) = -\beta(\mathbf{x} \cdot \hat{\mathbf{i}}) + P(\mathbf{x}, t), \quad (6)$$

where β is the value of the constant pressure gradient which decays along the streamwise direction and $P(\mathbf{x}, t)$ is the periodic component. This decomposition was used by Patankar et al. (1977), Murthy and Mathur (1997), and Beale (2007) to simulate unidirectional laminar flows spatially periodic under fully developed flow regime and it has been applied currently in two-phase modeling (see Sawko and Thompson (2011)).

In this work, we examine a flow whose hydrodynamics is both adiabatic and incompressible. In turn, the initial boundary value problem which we deal with is governed by the full dimensionless incompressible Navier-Stokes equations and we declare it by the following classical statement: find the pair (\mathbf{u}, P) , namely, the velocity and periodic pressure fields of the fluid flow, both defined over $\Omega \times \Theta$, for the time interval $\Theta = [0, t]$, which satisfy

$$\frac{D(\rho\mathbf{u})}{Dt} = \beta\hat{\mathbf{i}} - \nabla P + \frac{1}{Re}\nabla \cdot [\mu(\nabla\mathbf{u} + \nabla\mathbf{u}^T)] + \frac{1}{Fr^2}\rho\mathbf{g} + \frac{1}{We}\mathbf{f} \quad (7)$$

$$\nabla \cdot \mathbf{u} = 0 \quad (8)$$

with

$$\frac{D(\rho\mathbf{u})}{Dt} = \frac{\partial(\rho\mathbf{u})}{\partial t} + (\mathbf{u} - \hat{\mathbf{u}}) \cdot \nabla(\rho\mathbf{u}), \quad (9)$$

and the initial conditions given by

$$\mathbf{u}(\mathbf{x}, 0) = 0, \quad \text{for } \mathbf{x} \in \Omega \quad (10)$$

and the boundary conditions given by

$$\mathbf{u}|_{\Gamma_T} = \mathbf{u}|_{\Gamma_B} = -\mathbf{u}_l = (-u_l, 0), \quad \text{for } (0, t] \quad (11)$$

$$\mathbf{u}|_{\Gamma_L} = \mathbf{u}|_{\Gamma_R}, \quad \text{for } (0, t] \quad (12)$$

$$\left. \frac{\partial \mathbf{u}}{\partial \mathbf{n}} \right|_{\Gamma_R} = - \left. \frac{\partial \mathbf{u}}{\partial \mathbf{n}} \right|_{\Gamma_L}, \quad \text{for } (0, t] \quad (13)$$

$$P|_{\Gamma_L} = P|_{\Gamma_R} \quad \text{for } (0, t] \quad (14)$$

$$\left. \frac{\partial P}{\partial \mathbf{n}} \right|_{\Gamma_R} = - \left. \frac{\partial P}{\partial \mathbf{n}} \right|_{\Gamma_L}, \quad \text{for } (0, t] \quad (15)$$

$$P(\mathbf{x}_B, t) = 0, \quad \text{at } \mathbf{x}_B \in \Gamma_B, \text{ for } (0, t]. \quad (16)$$

Apart from the primitive variables appearing in Eqs. (7-8), ρ is the density of the fluid, $\hat{\mathbf{u}}$ is the *mesh velocity*, as seen in Donea et al. (2004), μ the dynamic viscosity of the fluid, \mathbf{g} a body force (here, the gravity field), Re the Reynolds number, Fr the Froude number, and We the Weber number. It should be noted that the term $-\beta \hat{\mathbf{i}}$ results from the application of the gradient operator on the both sides of the Eq. (6), whereby a vector with value constant in the streamwise component is obtained. In turn, the original unknown p is replaced with P , which is to be found. Furthermore, Eq. (11) means that the moving walls remain so along the time, whereas Eqs. (12-15) declare the PBC for velocity and pressure. The reference boundary condition for the pressure (16) is placed at a unique point \mathbf{x}_B over the lower wall.

According to the *one-fluid* formulation, Eqs. (7-8) hold in the interior of each phase apart and the force field \mathbf{f} congregates all the effects inherent to the interface. Following the idealization of integral force given by the Continuum Surface Model (CSF) by Brackbill et al. (1992), the force field \mathbf{f} is modeled as

$$\mathbf{f} = \sigma \kappa \nabla H, \quad (17)$$

where σ is the surface tension, κ the curvature, and H the Heaviside function defined according to

$$H(\mathbf{x}) := \begin{cases} 0, & \text{if } \mathbf{x} \in \Omega^l \\ 0.5, & \text{if } \mathbf{x} \equiv \mathbf{x}_I \in \Gamma_i^g, \quad \forall i = 1, 2, \dots, nb \\ 1, & \text{if } \mathbf{x} \in \Omega_i^g, \quad \forall i = 1, 2, \dots, nb. \end{cases} \quad (18)$$

The input parameters for the simulations are: the dynamic viscosities μ_k , the densities ρ_k , for $k = g, l$, the constant β (whenever a pressure gradient is desired), and the adimensional numbers.

3 METHODOLOGY

3.1 Design of Periodic Meshes

In order to implement PBC the meshes need to be designed to guarantee the correct spatial correspondence between the nodes belonging to the periodic boundaries Γ_L and Γ_R . Following Fritzen and Böhlke (2010), we will refer to the degrees of freedom (DOFs) of the periodic mesh as: *master*, *slave*, or *internal* accordingly their spatial location. The master DOFs will be those placed over the boundary chosen to be kept, whereas the slaves will be their opposite counterparts. All the remnant DOFs outside the periodic boundaries will be, hence, internal, even if they belong to nonperiodic boundaries. The master and slave nodes have different spatial coordinates on the mesh, but, in practice, they refer to the same DOF so that the slave DOFs are taken as “dummies” and their contribution is overloaded to the master DOFs.

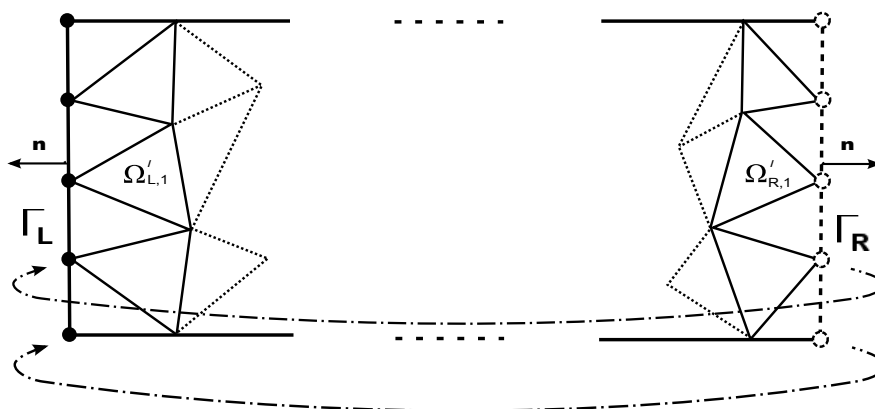


Figure 2: Geometrical sketch of the PBC implementation for a finite element mesh in two dimensions.

Figure 2 sketches the geometrical schematic to establish the PBC through the FEM over a two-dimensional domain. Γ_L , Γ_R are the master and slave periodic boundaries, respectively. Therefore, $\mathbf{x}_L = (x_L, y_L) \in \Gamma_L$ and $\mathbf{x}_R = (x_R, y_R) \in \Gamma_R$ are the master and slave nodes guarding the DOFs of interest. For γ nodes of discretization along the y -direction, the sequences

$$\begin{aligned} (\mathbf{x}_L; \gamma) &:= \{\mathbf{x}_{L,1}, \mathbf{x}_{L,2}, \dots, \mathbf{x}_{L,\gamma}\} \\ (\mathbf{x}_R; \gamma) &:= \{\mathbf{x}_{R,1}, \mathbf{x}_{R,2}, \dots, \mathbf{x}_{R,\gamma}\} \end{aligned}$$

define the geometrical periodicity of the mesh if $y_L = y_R$ for each node. This idea expands to tridimensional applications in a similar fashion. In Figure 2, $\Omega_{L,1}$ and $\Omega_{R,1}$ are the 1-ring neighbour elements of Γ_L and Γ_R , respectively, where we adapt the definition of “ k -rings” used by Wang et al. (2011) in order to establish a pairing between the two families of periodic elements. Thenceforth, the PBC are implemented via collapse of DOFs and modification of the original elementary equations (Segal et al. (1994), Nonino and Comini (1998)).

3.2 Finite Element Implementation

The pair of Eqs. (7-8) is discretized spatially by a mixed formulation which uses the stable MINI element, belonging to the Taylor-Hood’s family (see Arnold et al. (1984)) and the Galerkin’s method to approximate the function spaces. Given the suitable choices of function spaces, the Eqs. (7-8) are weighted and their variational formulation reached. All the mathematical details that lead to this weak form are minutely discussed in Temam (1977) and we will omit them here. After introducing approximations and applying the semi-discrete Galerkin’s method in the Navier-Stokes equations, symmetric matrices are obtained as well as a system discretized in space. Following the derivation presented by Anjos (2012), the finite element procedure for the two-phase model now transforms the original equations into the following discrete system:

$$\mathbf{M}_\rho \dot{\mathbf{u}} - \mathbf{M}\beta + \mathbf{G}\pi - \frac{1}{Re} \mathbf{K}\mathbf{u} - \frac{1}{Fr^2} \mathbf{M}_\rho \mathbf{g} - \frac{1}{We} \Sigma \mathbf{G}\mathbf{h} = \mathbf{0} \quad (19)$$

$$\mathbf{D}\mathbf{u} = \mathbf{0}, \quad (20)$$

where: \mathbf{M}_ρ is a mass matrix storing the contributions due to the differences of density; $\dot{\mathbf{u}}$ the discrete material derivative; \mathbf{M} another mass matrix, but relative to the contribution of the

nonperiodic part of the pressure which acts on the liquid phase only; $\beta = \beta \hat{\mathbf{i}}$ the vector storing the constant value of the streamwise pressure gradient; \mathbf{K} the matrix associated to the viscous term; \mathbf{u} the velocity vector; \mathbf{G} the matrix of the gradient operating on the periodic part of the pressure and on the Heaviside function vector \mathbf{h} ; $\boldsymbol{\pi}$ the vector of the periodic pressure field; $\boldsymbol{\Sigma} = \sigma \kappa(\mathbf{x}_I) \mathbf{I}$, with \mathbf{I} the identity matrix, the matrix storing the surface tension and curvature effects for each node at the interface, and \mathbf{D} the matrix of the divergence term.

Consecutively, for the temporal discretization, a Semi-Lagrangian method is undertaken to handle the material derivative, thus treating all the convective events by a backward-in-time integration, which pursues the trajectory of the fluid particles efficiently and affords better numerical stability requirements. Variants of this method are discussed in Staniforth and Côté (1991) and Xiu and Karniadakis (2001), while interpolation techniques are being developed by Oliveira et al. (2011), Oliveira et al. (2012). When discretizing the time t in $n = 0, 1, \dots, N$ time steps, the material derivative is approximated by

$$\dot{\mathbf{u}} = \frac{D\mathbf{u}}{Dt} \approx \frac{\mathbf{u}^{n+1}(\mathbf{x}) - \mathbf{u}^n(\mathbf{x}_d)}{\Delta t}, \quad (21)$$

where \mathbf{x}_d is called “departure point”. The remaining terms are treated explicitly. In turn, the system is treated as the following format:

$$\left(\frac{1}{\Delta t} \mathbf{M}_\rho + \frac{1}{Re} \mathbf{K} \right) \mathbf{u}^{n+1} + \mathbf{G} \boldsymbol{\pi}^{n+1} = \frac{1}{\Delta t} \mathbf{M}_\rho \mathbf{u}_d^n + \mathbf{M} \beta^* + \frac{1}{We} \boldsymbol{\Sigma} \mathbf{G} \mathbf{h}^n \quad (22)$$

$$\mathbf{D}^{n+1} = \mathbf{0}. \quad (23)$$

The superscript $*$ is to indicate that β does not change with the time. Next, Eqs. (22) and (23) are uncoupled, whereby it follows that

$$\begin{bmatrix} \mathbf{B} & \Delta t \mathbf{G} \\ \mathbf{D} & \mathbf{0} \end{bmatrix} \begin{bmatrix} \mathbf{u}^{n+1} \\ \boldsymbol{\pi}^{n+1} \end{bmatrix} = \begin{bmatrix} \mathbf{r}_d^n \\ \mathbf{0} \end{bmatrix} + \begin{bmatrix} \mathbf{bc}_1 \\ \mathbf{bc}_2 \end{bmatrix} + \Delta t \begin{bmatrix} \mathbf{M} \beta^* \\ \mathbf{0} \end{bmatrix} + \frac{\Delta t}{We} \begin{bmatrix} \boldsymbol{\sigma} \\ \mathbf{0} \end{bmatrix} \quad (24)$$

after multiplication by Δt and arrangement in a compact matricial form. Moreover, $\mathbf{B} = \mathbf{M}_\rho + \frac{\Delta t}{Re} \mathbf{K}$, $\mathbf{r}_d^n = \mathbf{M}_\rho \mathbf{u}_d^n$, and $\boldsymbol{\sigma} = \boldsymbol{\Sigma} \mathbf{G} \mathbf{h}^n$. The terms \mathbf{bc}_1 and \mathbf{bc}_2 account for boundary conditions for the velocity and pressure fields, respectively. Finally, the Eq. (24) is solved by using the projection method by Chorin (1968) & Temam (1969) after LU factorization of the matrix on the left hand side (Lee et al. (2001)) and application of substeps to correct the pressure and velocity fields, as inherent to the projection method.

4 NUMERICAL RESULTS AND DISCUSSION

This section presents a numerical simulation of the periodic array of bubbles with the MFR technique and imposition of PBC according to the previous framework. The case of study considers two bubbles whose geometry is pertinent to those found in Taylor flows for an air/water flow relative to a channel with diameter equivalent to $D = 50 \mu m$. For the simulation, the following values of fluid properties and flow conditions were prescribed: $\mu_l = 1.002 \times 10^{-3} Pa.s$, $\mu_g = 1.82 \times 10^{-5} Pa.s$, $\rho_l = 998.63 kg/m^3$, $\rho_g = 1.205 kg/m^3$, $\sigma = 0.0728 N/m$, $\beta = 10^{-4} Pa/m$, and $u_l = -0.2927 m/s$. These data yield $Re = 14.57$, $We = 0.20$, and $\delta = 0.079D$. For this problem, gravity effects were neglected. Figure 3 depicts a snapshot of the transient solution of the Heaviside function over the computational mesh identifying the bubbles at a particular instant. Vectors of the velocity field are plotted in Fig. 4, whose colors represent the scalar magnitude of the streamwise component. The application of the moving-frame

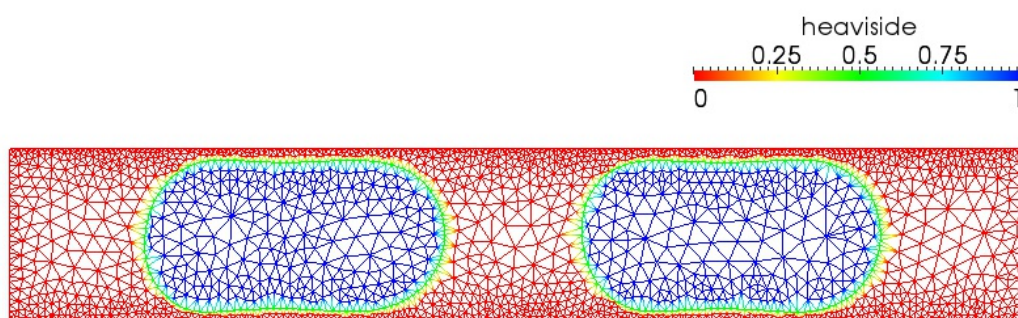


Figure 3: Heaviside function identifying the domain of the phases as well as the bubble's interfaces.

technique is demonstrated through the backward movement of the fluid flow imposed on the walls. Due to the higher refinement near the thin film region, consequent clustering of vectors is observed there. A parabolic profile develops on the both sides of the periodic boundaries and oppose to the direction of the velocity on the moving walls and recirculation zones are slightly concentrated near the fronts of bubble's interfaces. With the advance of the simulation and the remeshing process, the bubble's interfaces are displaced and some sites around the bubble's tail acquire a high velocity. Since the film thickness between the bubbles and the walls of the domain remains very small with the time, the movement of nodes over those regions tends to push the interface against the walls. In response to this event, some portion of liquid is squeezed and expelled out with a higher velocity. The pressure field is depicted in Fig. 5, where one

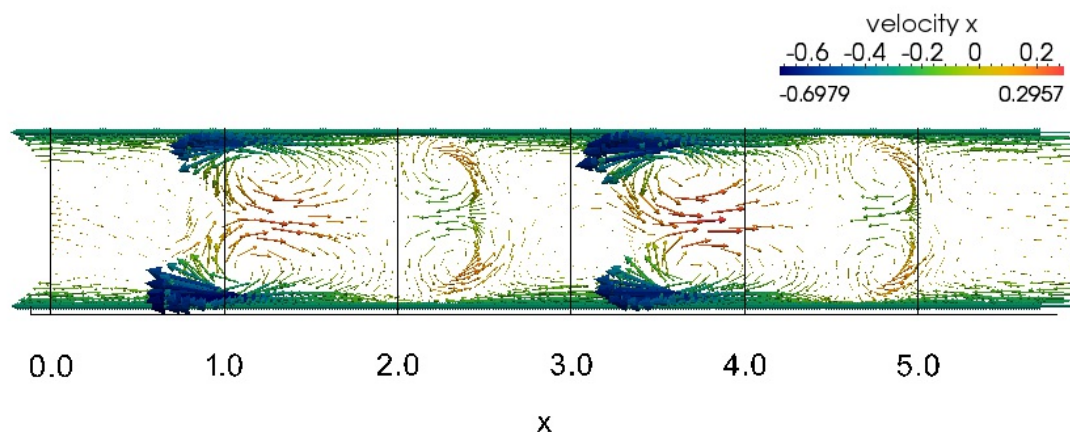


Figure 4: Vectors of the velocity field \mathbf{u} for the air/water flow.

observes a higher incidence of it on the bubbles and on the thin film region around them. Oscillations stemming from the numerical discretization are exhibited at the points near the interface, where the property changes abruptly. As a matter of fact, all the profiles are slightly deprived of smoothness at a few points because of discretization, as well as a poor refinement of mesh.

Graphs containing profiles of the streamwise component of the axial and mesh velocities, as well as the periodic pressure profile are plotted in Fig. 6. The constant functions in red appearing in each plot show, as expected, that the values of the fields match at the extreme points due to the PBC. High jumps of positive pressure are, *de facto*, found along the sites occupied by the bubbles, ascertaining the consistent physical representation brought out by the computational code.

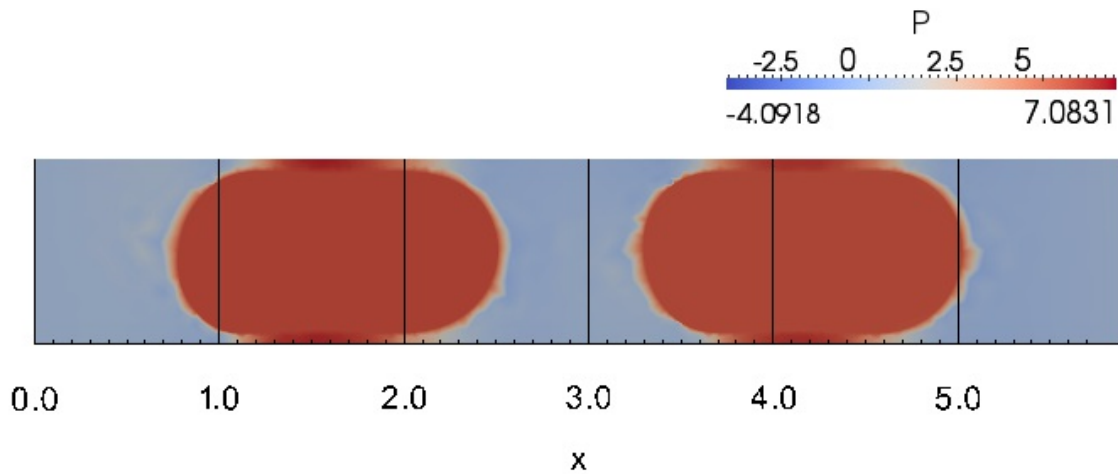


Figure 5: Surface plotting of the pressure field P for the air/water flow.

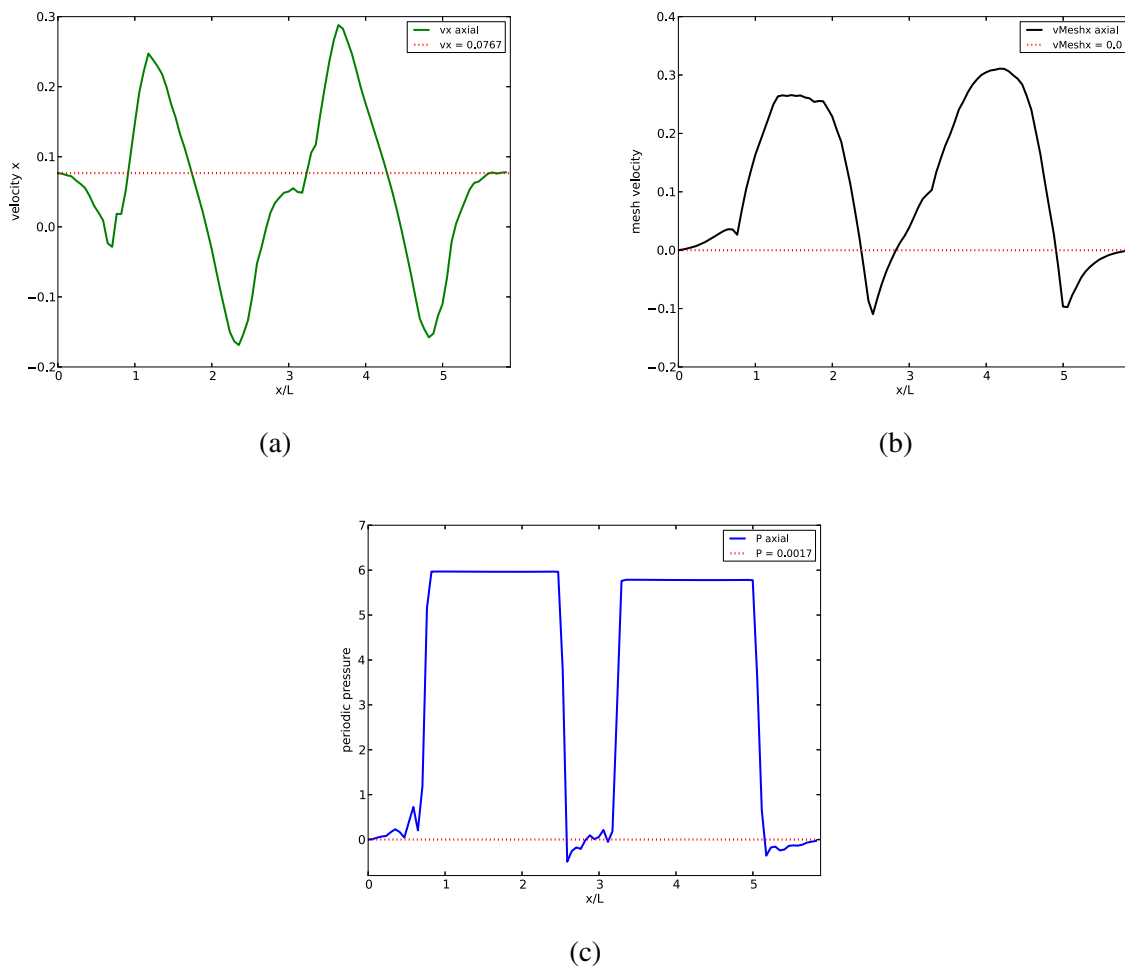


Figure 6: Profiles of the streamwise velocities and periodic pressure plotted along the axial direction of the periodic array: (a) velocity; (b) mesh velocity; (c) periodic pressure.

5 CONCLUSION

This paper analyzed the implementation of a methodology ALE/FE for two-phase flows by means of the imposition of periodic boundary conditions combined with a moving-frame technique into a relatively idealized problem, but with its physical parameters potentially relevant. We understand that the periodic array of bubbles is a convenient setup to study slug flows and capture its overall hydrodynamic effects, mainly due to the interaction of bubbles through and with the liquid slug separating them.

Periodic boundary conditions were included in the study to permit localized analyses of the flow and to avoid severe computational efforts. Their implementation through FEM is ruled by a topological connection based on the linkage of elements and provided a good numerical capability to handle simulations in smaller domains. Besides, this strategy serves further more complex cases and is being developed for application in tridimensional fluid flows, showing itself useful to simulate two-phase flows with an enriched dynamics.

Weak points exist since the modeling was performed within an adiabatic framework while in real applications the thin film thickness may be strongly influenced by its eaporation. Careful validations and verifications need to be addressed in order to strengthen the efficiency of the numerical code and enlarge its range of applicability for real situations. Nonetheless, these shortcomings are in active rectification by the authors. The next steps of this work lie on the application of these strategies in the periodic modeling of axisymmetric single-phase flows, annular two-phase flows, and then coupling these models with thermal effects.

ACKNOWLEDGMENT

G.C.P.O would like to thank CNPq - Conselho Nacional de Desenvolvimento Científico e Tecnológico, Brazil, for the sponsorship (Grant/Process: 238089-2012/6).

REFERENCES

- Anjos G., Mangiacavchi N., Borhani N., and Thome J. 3d ale finite element method for two-phase flows with phase change. *Heat Transfer Engineering*, Accepted for publishing, 2013.
- Anjos G.R. *A 3D ALE Finite Element Method for Two-Phase Flows with Phase Change*. Ph.D. thesis, EPFL - École Polytechnique Fédéral de Lausanne, Switzerland, 2012.
- Arnold D., Brezzi F., and Fortin M. A stable finite element for the stokes equations. *Calcolo*, 21(4):337–344, 1984.
- Asadolahi A.N., Gupta R., Fletcher D., and Haynes B. Cfd approaches for the simulation of hydrodynamics and heat transfer in taylor flow. *Chemical Engineering Science*, 66(22):5575–5584, 2011.
- Beale S. Use of streamwise periodic boundary conditions for problems in heat and mass transfer. *Journal of heat transfer*, 129(4):601–605, 2007.
- Brackbill J., Kothe D.B., and Zemach C. A continuum method for modeling surface tension. *Journal of computational physics*, 100(2):335–354, 1992.
- Bretherton F.P. The motion of long bubbles in tubes. *Journal of Fluid Mechanics*, 10(2):166–188, 1961.
- Campbell C. and Brennen C. Chute flows of granular material: some computer simulations. *Journal of applied mechanics*, 52(1):172–178, 1985.
- Chorin A.J. Numerical solution of the navier-stokes equations. *Mathematics of computation*, 22(104):745–762, 1968.
- Davies R.M. and Taylor G. The mechanics of large bubbles rising through extended liquids and

- through liquids in tubes. In *Proceedings of the Royal Society of London. Series A. Mathematical and Physical Sciences*. 1950.
- Donea J., Huerta A., Ponthot J.P., and Rodríguez-Ferran A. Arbitrary lagrangian–eulerian methods. *Encyclopedia of computational mechanics*, 2004.
- Fritzen F. and Böhlke T. Influence of the type of boundary conditions on the numerical properties of unit cell problems. *Technische Mechanik*, 30(4):354–363, 2010.
- Gupta R., Fletcher D., and Haynes B. On the cfd modelling of taylor flow in microchannels. *Chemical Engineering Science*, 64(12):2941–2950, 2009.
- Gupta R., Fletcher D., and Haynes B. Cfd modelling of flow and heat transfer in the taylor flow regime. *Chemical Engineering Science*, 65(6):2094–2107, 2010.
- Lee M.J., Byung D.O., and Young B.K. Canonical fractional-step methods and consistent boundary conditions for the incompressible navier–stokes equations. *Journal of Computational Physics*, 168(1):73–100, 2001.
- Magnini M. *CFD modeling of two-phase boiling flows in the slug flow regime with an interface capturing technique*. Ph.D. thesis, Università di Bologna, Italy, 2012.
- Magnini M., Pulvirenti B., and Thome J. Numerical investigation of the influence of leading and sequential bubbles on slug flow boiling within a microchannel. *International Journal of Thermal Sciences*, 71:36–52, 2013.
- Maury B. Direct simulations of 2d fluid-particle flows in biperiodic domains. *Journal of computational physics*, 156(2):325–351, 1999.
- Murthy J. and Mathur S. Periodic flow and heat transfer using unstructured meshes. *International journal for numerical methods in fluids*, 25(6):659–677, 1997.
- Nonino C. and Comini G. Finite-element analysis of convection problems in spatially periodic domains. *Numerical Heat Transfer, Part B*, 34(4):361–378, 1998.
- Oliveira G., Mangiavacchi N., and Pontes J. A semi-lagrangian scheme for fluid flow simulations with a zienkiewicz-type finite element interpolation. In *21st International Congress of Mechanical Engineering*. 2011.
- Oliveira G., Mangiavacchi N., and Pontes J. Semi-lagrangian high-order 3d interpolation: Survey on a finite element z-type operator. In *14th Brazilian Congress of Thermal Sciences and Engineering*. 2012.
- Patankar S., Liu C., and Sparrow E. Fully developed flow and heat transfer in ducts having streamwise-periodic variations of cross-sectional area. *Journal of Heat Transfer*, 99:180, 1977.
- Sawko R. and Thompson C.P. Towards multiphase periodic boundary conditions with flow rate constraint. In *AIP Conference Proceedings*, volume 1389, page 147. 2011.
- Segal G., Vuik K., and Kassels K. On the implementation of symmetric and antisymmetric periodic boundary conditions for incompressible flow. *International journal for numerical methods in fluids*, 18(12):1153–1165, 1994.
- Staniforth A. and Côté J. Semi-lagrangian integration schemes for atmospheric models—a review. *Monthly Weather Review*, 119(9):2206–2223, 1991.
- Talimi V., Muzychka Y.S., and Kocabiyik S. Numerical simulation of the pressure drop and heat transfer of two phase slug flows in microtubes using moving frame of reference technique. *International Journal of Heat and Mass Transfer*, 55:6463–6472, 2012a.
- Talimi V., Muzychka Y.S., and Kocabiyik S. A review on numerical studies of slug flow hydrodynamics and heat transfer in microtubes and microchannels. *International Journal of Multiphase Flow*, 39:88–104, 2012b.
- Temam R. Sur l’approximation de la solution des équations de navier-stokes par la méthode des

- pas fractionnaires (i). *Archive for Rational Mechanics and Analysis*, 32(2):135–153, 1969.
- Temam R. *Navier-Stokes equations: theory and numerical analysis*, volume 1. North-Holland, 1977.
- Wang W., Zhang Y., Scott M.A., and Hughes T.J. Converting an unstructured quadrilateral mesh to a standard t-spline surface. *Computational Mechanics*, 48(4):477–498, 2011.
- Xiu D. and Karniadakis G. A semi-lagrangian high-order method for navier-stokes equations. *Journal of Computational Physics*, 172(2):658–684, 2001.